Rate Constant for the $NH_3 + NO_2 \rightarrow NH_2 + HONO$ Reaction: Comparison of Kinetically Modeled and Predicted Results

A. GRANT THAXTON, C.-C. HSU, M. C. LIN

Department of Chemistry, Emory University, Atlanta, Georgia 30322

Received 28 May 1996; accepted 22 July 1996

ABSTRACT: The rate constant for the $NH_3 + NO_2 \rightleftharpoons NH_2 + HONO$ reaction (1) has been kinetically modeled by using the photometrically measured NO_2 decay rates available in the literature. The rates of NO_2 decay were found to be strongly dependent on reaction (1) and, to a significant extent, on the secondary reactions of NH_2 with NO_x and the decomposition of HONO formed in the initiation reaction. These secondary reactions lower the values of k_1 determined directly from the experiments. Kinetic modeling of the initial rates of NO_2 decay computed from the reported rate equation, $-d[NO_2]/dt = k_1[NH_3][NO_2]$ based on the conditions employed led to the following expression:

$$k_1 = 10^{11.39 \pm 0.16} e^{-(12620 \pm 240)/T} cm^3 mole^{-1} s^{-1}$$

This result agrees closely with the values predicted by ab initio MO [G2M//B3LYP/6-311G(*d*,*p*)] and TST calculations. © 1997 John Wiley & Sons, Inc. Int J Chem Kinet **29:** 245–251, 1997.

INTRODUCTION

The thermal reaction of NH_3 with NO_2 is kinetically relevant to the deNO_x process [1–4] as well as to the combustion of ammonium nitrate (AN) and ammonium dinitramide (ADN) [5–7]. The reaction has been investigated earlier by Rosser and Wise [8] and by Bedford and Thomas [9]. Both groups attributed the initial decay of NO_2 measured photometrically to the bimolecular reaction:

$$NH_3 + NO_2 \longrightarrow NH_2 + HONO \qquad (1)$$

Rosser and Wise derived the expression, $k_1' = 5 \times 10^{12}\ e^{-13840/T}\ cm^3\ mole^{-1}\ s^{-1}$, for the temperature range of 600–800 K, with no mechanistic details or interpretation. Bedford and Thomas [9] attempted to analyze their kinetic data obtained in a narrower temperature range of 615–660 K in terms of a mechanism containing both NH and NH_2 radical reactions. Under the low temperature conditions employed, however, the involvement of the NH radical is unrealistic on the basis of the heat of formation of the radical known today [10]. Their apparent second-order rate constant could be represented by $k_1' = 8 \times 10^{12}\ e^{-13920/T}\ cm^3\ mole^{-1}\ s^{-1}$, which is in reasonable agreement with that of Rosser and Wise given above. These results, however, may be affected by the fast

Correspondence to: M. C. Lin
Contact grant Sponsor: Office of Naval Research
Contact grant number: N00014-89-J-1949
 CCC 0538-8066/97/040245–07

chain reactions involving NH_2 and NO_x which produce highly reactive radicals such as H and OH.

In a recent flow study by Glarborg and co-workers [11] on the reduction of NO_2 by NH_3 the authors used an estimate for the reverse of reaction (1), $NH_2 + HONO \rightarrow NH_3 + NO_2$, $k_{-1} = 5 \times 10^{12}$ cm^3 mole^{-1} s^{-1}, which was considered to be consistent with the values of k_1' mentioned above.

In view of the great reactivity of NH_2 toward NO_2 and the complexity of the $NH_3 + NO_2$ system, we have carried out kinetic modeling of the initial decay of NO_2 measured by Rosser and Wise [8] and Bedford and Thomas [9] using our recently measured product branching ratio for the $NH_2 + NO_2$ reaction [12] which allows us to realistically simulate subsequent secondary reactions involving NO_2. The results of this modeling reveal that the initial decay of NO_2 was indeed controlled to a large extent by reaction (1) and the effect of secondary reactions on the reported decay rates is quite pronounced also.

In the following sections, we describe the procedure and kinetic data used in our modeling and the modeled values of k_1 are compared with our quantum-chemically predicted results.

KINETIC MODELING

NO_2 Decay Data

The initial rates of NO_2 decay measured photometrically by Rosser and Wise [8] and Bedford and Thomas [9] can be computed by their experimentally determined second-order rate equation:

$$-d[NO_2]/dt = k_1'[NH_3][NO_2] \qquad (1)$$

Table I Kinetic Data of Rosser and Wise[a] and Modeled Values of k_1[b]

T(K)	P_{NH_3} (torr)	P_{NO_2} (torr)	$-d[NO_2]/dt$[d]	time (s)[c]	k_1
793.7	247.6	.99	38.63	.0695	32500
787.4	98.3	2.46	29.48	.226	28000
740.7	277.3	3.70	35.94	.282	7800
715.1	401.6	4.02	36.86	.297	5600
708.3	88.4	.88	11.73	.390	5450
710.5	354.7	1.77	13.02	.378	4450
719.6	179.6	3.59	12.93	.765	5100
710.2	221.6	.89	3.19	.750	3750
705.7	220.2	2.20	7.26	.827	3850
697.8	217.7	.87	3.11	.760	3800
693.2	129.8	2.60	15.56	.285	4550
709.6	265.7	1.33	4.54	.81	3050
692.4	388.9	3.89	20.98	.505	3500
658.6	369.9	3.67	6.59	1.53	1260
659.0	205.6	2.06	1.91	2.93	1180
652.6	122.2	2.85	1.59	4.72	1200
647.5	323.2	2.42	2.56	2.59	850
640.2	319.6	2.40	2.19	3.00	745
626.9	156.5	1.17	.307	10.3	435
625.0	117.0	1.56	.281	15.2	370
625.0	312.0	2.73	1.14	6.48	350
616.1	269.1	3.08	1.06	7.70	330
604.5	264.0	1.89	.388	13.2	200
604.5	188.6	2.64	.372	18.5	195
598.1	74.6	1.12	.066	48.2	200
600.3	112.4	.75	.058	35.0	175
598.7	261.5	2.62	.439	16.3	165
598.1	261.3	2.61	.417	17.1	157
571.4	285.3	3.21	.200	43.2	58

[a] Ref. [8].

[b] Rate constant is given in units of cm^3 mole^{-1} s^{-1}.

[c] The duration of reaction leading to conversion of approximately 4.5%.

[d] Initial rates of NO_2 decay in units of torr/min computed from the apparent second-order rate equation, $k_1'[NH_3][NO_2]$ using their reported values of k_1', transcribed directly from the original figure.

Table II Kinetic Data of Bedford and Thomas[a] for the Effects of Temperature and Added NO and our Modeled Values of k_1[b]

T(K)	P_{NO} (torr)	$-d[NO_2]/dt$[c]	k_1
619	0.0	.501	420
	1.54	.481	445
	3.08	.427	365
	5.54	.391	345
	7.38	.350	360
	26.2	.253	320
	43.0	.233	340
	61.0	.203	335
	73.0	.195	345
	100.7	.186	390
630	0.0	.761	615
639	0.0	1.06	865
648	0.0	1.36	1110
657	0.0	1.76	1440

[a] Ref. [9].

[b] Rate constant is given in units of $cm^3\ mole^{-1}\ s^{-1}$. The initial pressures of NH_3 and NO_2 used in the modeling were 44.0 and 6.1 torr, respectively, as employed in their NO-inhibited experiment [9].

[c] The initial rates of NO_2 decay, given in units of torr/mm, were computed with the rate equation, $k_1'[NH_3][NO_2]$, using the reported values of k_1', or $-d[NO_2]/dt$ in the NO-inhibited case, in their original figures.

using the values of rate constants directly transcribed from their original figures and the experimental conditions stated in their articles. The calculated initial rates, presented in Tables I and II, were kinetically modeled for k_1 using the mechanism presented in Table III.

In our modeling, we limited the conversion of NO_2, $([NO_2]_0 - [NO_2]_t)/[NO_2]_0$, to less than 4.5% so as to minimize the effect of secondary reactions. In theory, the decay rates at any conversions can be readily calculated by kinetic modeling. However, a much smaller value than 3–5% may not be realistically measured experimentally.

Ab Initio MO and TST Calculations

Recently, we have calculated the rate constants for the reactions of NH_3 with NO_x [13]:

$$NH_3 + NO \longrightarrow NH_2 + HNO$$

$$NH_3 + NO_2 \longrightarrow NH_2 + HONO$$

using transition state (TS) and molecular parameters computed by the G2 [14] and G1 [15] methods, respectively. A detailed description of the potential energy surfaces and reaction characteristics of these processes can be found in ref. [13]. The theoretically predicted results for reaction (1) will be compared with our kinetically modeled values of k_1 later.

In the present study, we utilized a modified G2 (or G2M) method, recently employed by Mebel, Morokuma, and Lin [16], to calculate the energetics of the reactants and the transition state identified in ref. [13] to compare with the modeled and calculated (G1) values. For the rate constant calculation, conventional TST was employed because of the existence of the well-defined TS [13].

RESULTS AND DISCUSSION

Reaction Mechanism

The initial rates of NO_2 decay, $-d[NO_2]/dt$, were kinetically modeled with the mechanism presented in Table III. The mechanism was established on the basis of our recent investigation of the $H_2 + NO$ and $NH_y + NO_x$ (x = 1,2; y = 2,3) reactions employing the pyrolysis/FTIR spectrometry [17,18] and laser-photolysis-mass spectrometric techniques [12,19], as well as other related studies which appeared in recent literature [4,11,20,22]. For the key processes with potential chain-branching capabilities such as

$$NH_2 + NO \longrightarrow N_2H + OH$$

$$NH_2 + NO_2 \longrightarrow H_2NO + NO$$

followed by

$$N_2H + M \longrightarrow H + N_2 + M$$

$$H_2NO + M \longrightarrow H + HNO + M$$

$$HNO + M \longrightarrow H + NO + M,$$

we used our latest product branching ratios determined for the $NH_2 + NO_x$ reactions [12,19,21].

The decay of NO_2 was found to be controlled primarily by reaction (1),

$$NH_3 + NO_2 \longrightarrow NH_2 + HONO \qquad (1)$$

however, with a significant effect by secondary reactions. The modeling of the reported initial rates of NO_2 by Rosser and Wise [8] and Bedford and Thomas [9], summarized in Tables I and II, respectively, yielded the values of k_1 which are smaller by a factor of 3–5 than those originally reported as shown in Figure 1. A weighted least-squares analysis of k_1 summarized in Tables I and II gave

$$k_1 = 10^{11.39 \pm 0.16}\, e^{-(12620 \pm 240)/T}\ cm^3\ mole^{-1}\ s^{-1}$$

covering the temperature range studied, 600–800 K. The combination of the k_1 expression with the equilibrium constant, $K_1 = 8.87\ e^{-15524/T}$ calculated with JANAF data [10] gave rise to the rate constant for the

Table III The Reactions and Rate Constants used in the Modeling of Existing Kinetic Data[a]

Reactions	A	B	C
1. $NH_3 + NO_2 = NH_2 + HONO$	2.211E11	0.0	24906.0
2. $NH_2 + NO_2 = H_2NO + NO$	8.83E11	0.11	− 1186.0[b]
3. $NH_2 + NO_2 = N_2O + H_2O$	2.07E11	0.11	− 1186.0[b]
4. $NH_2 + NO = N_2 + H_2O$	4.46E19	− 2.56	403.0[c]
5. $NH_2 + NO = NNH + OH$	1.75E12	− 0.33	− 968.0[c]
6. $HONO + M = OH + NO + M$	1.0E30	− 3.59	50170.0
7. $OH + NH_3 = H_2O + NH_2$	2.0E12	0.0	1832.0
8. $H_2NO + M = H + HNO + M$	1.28E38	− 6.42	72726.0[d]
9. $NNH + M = H + N_2 + M$	1.0E14	0.0	3000.0
10. $H + NH_3 = NH_2 + H_2$	6.36E5	2.39	10171.0
11. $H + NO_2 = OH + NO$	3.5E14	0.0	1500.0
12. $OH + NO_2 + M = HNO_3 + M$	3.6E47	− 5.49	2350.0
13. $NO_2 + NO_2 = 2NO + O_2$	8.6E12	0.0	28800.0
14. $NO_2 + NO_2 = NO_3 + NO$	3.2E12	0.0	25700.0
15. $HONO + HONO = NO + NO_2 + H_2O$	6.2E11	0.0	8186.0
16. $OH + NH_2 = O + NH_3$	2.0E10	0.4	497.0
17. $OH + NH_2 = NH + H_2O$	5.0E11	0.5	1980.0
18. $NH_3 + M = NH_2 + H + M$	2.2E16	0.0	93468.0
19. $N_2H_4 + M = NH_2 + NH_2 + M$	4.0E15	0.0	40932.0
20. $NH_2 + NH_2 = NH + NH_3$	5.0E13	0.0	10000.0
21. $NH + NO = N_2O + H$	1.4E14	0.0	12717.0
22. $NH + NO = N_2 + OH$	3.2E13	0.0	12717.0
23. $H + NO + M = HNO + M$	5.4E15	0.0	− 596.0
24. $H + NO = N + OH$	1.7E14	0.0	48800.0
25. $NH_3 + NO = NH_2 + HNO$	1.04E7	1.73	56538.0
26. $H_2NO + NO_2 = HNO + HONO$	1.0E12	0.0	0.0
27. $H_2NO + NO = HNO + HNO$	1.0E12	0.0	0.0
28. $NH_2 + H = NH + H_2$	4.0E13	0.0	3650.0
29. $HNO + HNO = N_2O + H_2O$	8.9E8	0.0	3100.0
30. $OH + HONO = H_2O + NO_2$	7.8E11	0.0	− 380.0
31. $H + OH + M = H_2O + M$	1.6E22	− 2.0	0.0
32. $OH + HNO = H_2O + NO$	1.3E7	1.9	− 958.0
33. $OH + OH = H_2O + O$	2.2E8	1.4	− 400.0
34. $OH + OH + M = H_2O_2 + M$	5.7E24	− 3.0	0.0
35. $NH_2 + O = NH + OH$	1.3E14	− 0.5	0.0
36. $NH_2 + O = HNO + H$	6.3E14	− 0.5	0.0
37. $H + H + M = H_2 + M$	5.0E18	− 1.0	0.0
38. $H + HNO = H_2 + NO$	4.5E11	0.72	650.0
39. $H + N_2O = OH + N_2$	1.55E-2	4.39	2891.0
40. $OH + H_2 = H_2O + H$	1.0E8	1.6	3300.0
41. $HNO + NO = OH + N_2O$	8.5E12	0.0	29586.4
42. $HNO + NO_2 = NO + HONO$	1.8E12	0.0	7130.0
43. $H_2NO + M = HNOH + M$	3.00E34	− 4.45	59940.0[d]
44. $HNO + HNO = HNOH + NO$	2.0E8	0.0	2100.0
45. $HNOH + M = H + HNO + M$	3.41E31	− 5.67	62072.0
46. $OH + H_2NO = H_2O + HNO$	7.8E11	0.0	− 300.0
47. $OH + HNOH = H_2O + HNO$	7.8E11	0.0	− 300.0

[a] The rate constant parameters used in the mechanism, defined by $k = AT^B e^{-c/RT}$ in units of cm^3/mole-s and R = 1.987 ca/mole-deg, were adopted in part from refs. [4,11,12,17,18,20–22].

[b] Ref. [12].

[c] Refs. [19] and [21].

[d] S. Kristyan, private communication.

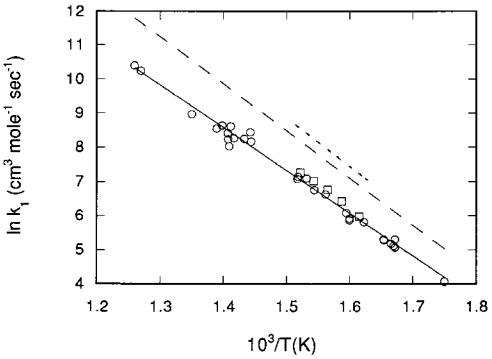

Figure 1 Comparison of kinetically modeled k_1 with that of Rosser and Wise [8] given by the dashed line and of Bedford and Thomas [9] given by the dotted line.

reverse process, $NH_2 + HONO \rightarrow NH_3 + NO_2$, $k_{-1} = 2.8 \times 10^{10}\, e^{2900/T}\, cm^3\, mole^{-1}\, s^{-1}$.

The lowering of the bimolecular rate constant from their original values [8,9] resulted directly from the participation of the fast secondary atomic and radical reactions mentioned above, most of which were not considered in the original kinetic analyses. The effects of some of these radical reactions are evident from the results of sensitivity analyses shown in Figure 2 (a) and (b). For example in the $NH_2 + NO_2$ reaction, the channel leading to the formation of H_2NO, which can decompose to give H + HNO as alluded to above, has a destructive effect on NO_2 with a negative sensitivity coefficient, whereas the channel leading to the formation of stable molecules, N_2O + H_2O, has an apparent "enhancement" effect with a positive sensitivity coefficient. Similarly, $HONO + M \rightarrow OH + NO + M$ and $2HONO \rightarrow NO + NO_2 + H_2O$ have opposite effects.

The importance of the $NH_2 + NO_2$ reaction is also illustrated by the strong NO-inhibition effect shown in Table II and Figure 3. The NO effect, which could be fully accounted for by the model, resulted from the participation of the NH_2 + NO reaction, giving rise to stable molecules, N_2 and H_2O, as primary products. At 700 K, 82% of the reaction generates these molecular products with the remaining 18% resulting in radical products, N_2H + OH [19]. The result of a sensitivity analysis shown in Figure 2 C for the NO-inhibited case nicely illustrates the retardation effect of the $NH_2 + NO \rightarrow N_2 + H_2O$ reaction of NO_2 with large positive sensitivity coefficients.

Comparison of Modeled k_1 with Theory

As alluded to in the preceding section, we have earlier calculated the rate constant for the $NH_3 + NO_2$ reaction by TST using the energies and molecular parameters computed at the G1//UMP2/6-311G(*d*,*p*) and G1//B3LYP/6-311G(*d*,*p*) levels of theory [13]. As shown in Figure 4, the value of the rate constant obtained by the former method was smaller than that obtained by the latter by a factor of 3, because of the tight transition state structure predicted by the MP2 theory in general. In this study, we carried out additional calculations with the G2M method which has been described in detail in ref. [16]. The energies computed by means of various methods are summarized in Table IV. The calculated heats of formation of individual reactants and products agree within

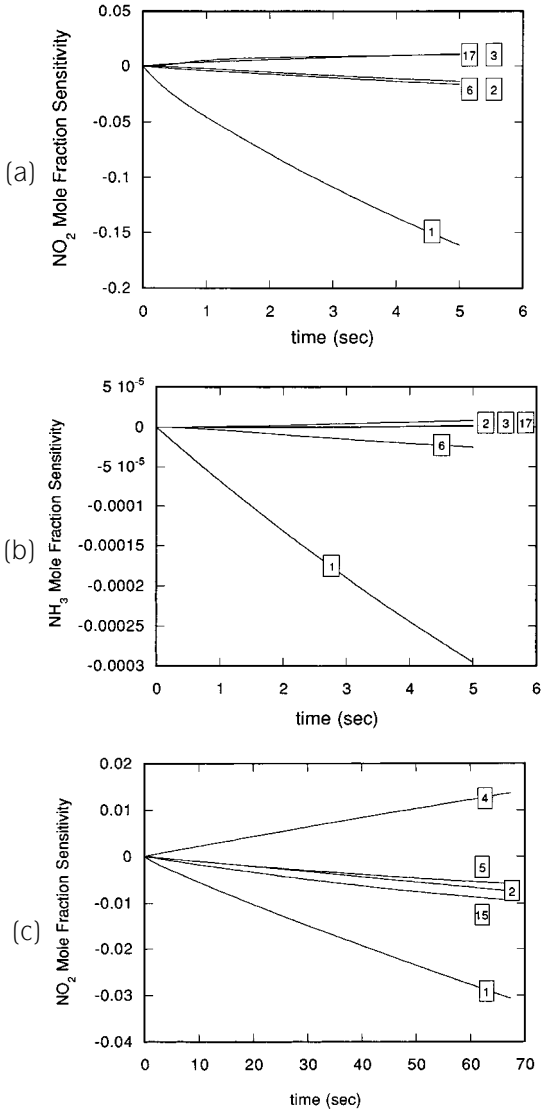

Figure 2 Sensitivity analysis for (a) NO_2, (b) NH_3, and (c) NO_2 with added NO. For (a) and (b): T = 698 K; P_{NO_2} = 0.87 torr; and P_{NH_3} = 218 torr; for (c): T = 619 K; P_{NO_2} = 6.1; P_{NH_3} = 44.0; and P_{NO} = 43.0 torr.

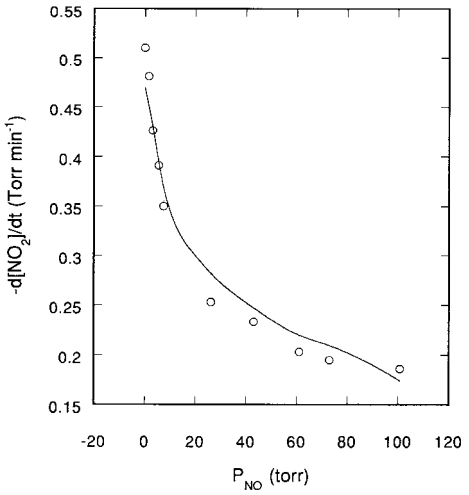

Figure 3 Effect of NO on the rates of NO_2 decay measured at 619 K by Bedford and Thomas [9]. Their data are summarized in Table II. The solid curve gives the calculated values.

2 kcal/mole with experimental values [10]. The reaction barriers obtained by the G1 and G2M methods agree within 0.5 kcal/mole and are in excellent agreement with the experimental activation energy, 25 ± 0.5 kcal/mole. The calculated absolute values of k_1 shown in Figure 4, particularly that based on the G2M//B3LYP/6-311G(*d*,*p*) level of theory, are also in good accord with the kinetically modeled results.

The transition state considered in the present calculation leads to the formation of *cis*-HONO. Two other potential channels,

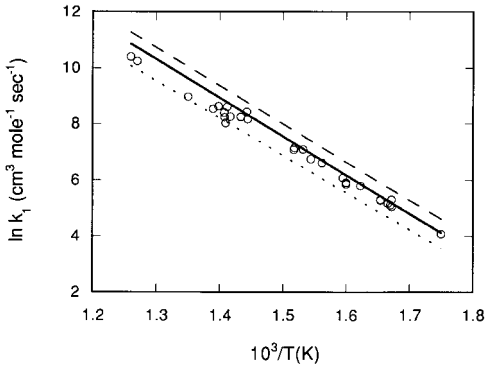

Figure 4 Comparison of kinetically modeled values of k_1 with those predicted by TST calculations based on various levels of MO theory. (Solid line) TST-G2M//B3LYP/6-311G(*d*,*p*), this work; (dotted line) TST-G1(PU)//UMP2/6-311G(*d*,*p*), ref. [13]; and (dashed line) TST-G1//B3LYP/6-311G(*d*,*p*), ref. [13] (this result has been reduced by a factor of 2 due to an input data error in the TST calculation).

$$NH_3 + NO_2 \longrightarrow NH_2 + \textit{trans}\text{-HONO}$$

$$NH_3 + NO_2 \longrightarrow NH_2 + HNO_2$$

were found to have higher reaction barriers by 9.9 and 7.2 kcal/mole, respectively, than that of the *cis*-HONO product channel at the G1(PU)//UMP2/6-311G(*d*,*p*) level of theory [13]. Therefore, the production of trans-HONO and HNO_2 below 1000 K is expected to be insignificant and can be ignored.

CONCLUSION

Experimentally measured rates of NO_2 decay by Rosser and Wise [8] and by Bedford and Thomas [9] have been kinetically modeled with sensitivity analyses using our recently determined product branching ratios for the $NH_2 + NO_x$ (x = 1,2) reactions [12,19]. The decay of NO_2 was found to be strongly dependent on the initiation reaction (1), $NH_3 + NO_2 \rightarrow NH_2 + HONO$, and to a significant extent, on the effects of secondary reactions involving NH_2 and NO_x and the decomposition of HONO which produces the most reactive chain carrier, OH. Our kinetically modeled results can be effectively represented by $k_1 = 2.5 \times 10^{11}\ e^{-12620/T}\ cm^3\ mole^{-1}\ s^{-1}$. These results are lower by a factor of 3–5 than the second-order rate constants reported by the original authors, attributable to the aforementioned secondary reactions. However, the modeled values of k_1 are in good accord with our theoretically predicted results by ab initio MO/TST calculations.

The authors gratefully acknowledge the support of this work by the Office of Naval Research (contract no. N00014-89-J-1949) under the direction of Dr. R. S. Miller. We thank the Cherry L. Emerson Center for Scientific Computation for the use of computing facilities and various programs.

BIBLIOGRAPHY

1. R. K. Lyon, *Int. J. Chem. Kinet.*, **8,** 318 (1976); U.S. Patent 3,900,554.
2. J. A. Miller, M. C. Branch, and R. J. Kee, *Combust. Flame*, **43,** 81 (1981).
3. J. A. Miller and C. T. Bowman, *Prog. Energy Combust. Sci.*, **15,** 287 (1989).
4. P. Glarborg, K. Dam-Johansen, J. A. Miller, R. J. Kee, and M. E. Coltrin, *Int. J. Chem. Kinet.*, **26,** 421 (1994).

Table IV Relative Energies (kcal/mol) of Various Species, Calculated with the G1(PU) and G2M Methods

Species	UMP2/6-311 G(*d*,*p*) + ZPE[a]	B3LYP/6-311 G(*d*,*p*) + ZPE[a]	G1(PU)[b]	G2M[c]	exp[d]
$NH_3 + NO_2$[e]	0.0	0.0	0.0	0.0	0.0
TS	39.6	20.1	24.6	25.0	
NH_2 + *cis*-HONO	33.0	31.5	27.3	26.5	30.1

[a] Zero-point energies calculated at the UMP2/6-311G(*d*,*p*) level were scaled by 0.95, whereas those calculated at B3LYP/6-311G(*d*,*p*) were used without scaling.

[b] G1(PU) energies were based on the UMP2/6-311G(*d*,*p*) optimized geometries (see ref. [13]).

[c] G2M energies were based on the B3LYP/6-311G(*d*,*p*) optimized geometries, this work.

[d] The JANAF table, ref. [10].

[e] The total energies computed by the four levels of theory are given in sequence: − 261.02262, − 261.66901, − 261.28303, and − 261.31662 hartree.

5. T. B. Brill, P. J. Brush, and D. G. Patil, *Combust. Flame,* **92,** 7788 (1993).
6. M. J. Rossi, J. C. Bottaro, and D. F. McMillen, *Int. J. Chem. Kinet.*, **25,** 549 (1993).
7. A. M. Mebel, M. C. Lin, K. Morokuma, and C. F. Melius, *J. Phys. Chem.*, **99,** 6842 (1995).
8. W. A. Rosser, Jr. and H. Wise, *J. Chem. Phys.*, **29,** 1078 (1956).
9. G. Bedford and J. H. Thomas, *JCS Faraday Trans. I,* **68,** 2163 (1972).
10. W. M. Chase, Jr., C. A. Davies, J. R. Downey, Jr., D. J. Frurip, R. A. McDonald, and A. N. Syverud, *J. Phys. Chem. Ref. Data,* **14,** (Suppl.) 1 (1995).
11. P. Glarborg, K. Dam-Johansen, and J. A. Miller, *Int. J. Chem. Kinet.*, **27,** 1207 (1995).
12. J. Park and M. C. Lin, *Int. J. Chem. Kinet.*, in press.
13. A. M. Mebel, E. W. G. Diau, M. C. Lin, and K. Morokuma, *J. Phys. Chem.*, **100,** 7517 (1996).
14. J. A. Pople, M. Head-Gordon, D. J. Fox, K. Raghavachari, and L. A. Curtiss, *J. Chem. Phys.*, **90,** 5622 (1989).
15. L. A. Curtiss, K. Raghavachari, G. W. Trucks, and J. A. Pople, *J. Chem. Phys.*, **94,** 7221 (1991).
16. A. M. Mebel, K. Morokuma, and M. C. Lin, *J. Chem. Phys.*, **103,** 7414 (1995).
17. E. W. G. Diau, M. J. Halbgewachs, A. R. Smith, and M. C. Lin, *Int. J. Chem. Kinet.*, **27,** 867 (1995).
18. M. J. Halbgewachs, E. W. G. Diau, M. C. Lin, and C. F. Melius, *26th Symp. of Combust.*, accepted.
19. J. Park and M. C. Lin, *J. Phys. Chem.*, **100,** 3317 (1996).
20. E. W. G. Diau, M. C. Lin, Y. He, and C. F. Melius, *Prog. in Energy and Combust. Sci.*, **21,** 1 (1995).
21. J. Park and M. C. Lin, *J. Phys. Chem.*, submitted.
22. W. Tsang and J. T. Herron, *J. Phys. Chem. Ref. Data,* **20,** 609 (1991).